

Particle Propagation in the Galactic Center and Spatial Distribution of Non-Thermal X-rays

Vladimir DOGIEL^{1,2}, Dmitrii CHERNYSHOV^{2,3}, Takayuki YUASA⁴, Kwong-Sang CHENG⁵, Aya BAMBA¹, Hajime INOUE¹, Chung-Ming KO⁶, Motohide KOKUBUN¹, Yoshitomo MAEDA¹, Kazuhisa MITSUDA¹, Kazuhiro NAKAZAWA⁴, and Noriko Y. YAMASAKI¹

¹*Institute of Space and Astronautical Science, 3-1-1, Yoshinodai, Sagamihara, Kanagawa, 229-8510, Japan*

²*P.N.Lebedev Institute, Leninskii pr, 53, 119991 Moscow, Russia, dogiel@lpi.ru*

³*Moscow Institute of Physics and Technology, Institutskii lane, 141700 Moscow Region, Dolgoprudnii, Russia*

⁴*Department of Physics, School of Science, The University of Tokyo, 7-3-1 Hongo, Bunkyo-ku, Tokyo 113-0033*

⁵*Department of Physics, University of Hong Kong, Pokfulam Road, Hong Kong, China*

⁶*Institute of Astronomy, National Central University, Jhongli 320, Taiwan*

(Received 2000 December 31; accepted 2001 January 1)

Abstract

We showed that if the non-thermal emission from the Galactic center in the range 14 – 40 keV is due to inverse bremsstrahlung emission of subrelativistic protons, their interactions with hot and cold fractions of the interstellar medium are equally important. Our estimation show that about 30% of the total non-thermal flux from the GC in the range 14 – 40 keV is generated in regions of cold gas while the rest is produced by proton interaction with hot plasma. From the spatial distribution of 6.7 keV iron line we concluded the spatial distribution of hot plasma is strongly non-uniform that should be taken into account in analysis of protons propagation in the GC. From the Suzaku data we got independent estimates for the diffusion coefficient of subrelativistic protons in the GC, which was in the range $10^{26} - 10^{27} \text{ cm}^2\text{s}^{-1}$

Key words: Galaxy: center - X-rays: diffuse background - ISM: cosmic rays

1. Introduction

This is a final paper of the series (Cheng et al. 2006; Cheng et al. 2007; Dogiel et al. 2008; Dogiel et al. 2009abc) on energetic processes in the Galactic center (GC). In these papers we presented our interpretation of X-ray and gamma-ray emission from the Galactic center.

We supposed that all these phenomena had common origin and were initiated by accretion processes onto the central supermassive black hole.

We showed that the the observed X-ray continuum and line emission from the GC might be produced by a flux of subrelativistic protons which resulted from an unbounded part of stars accreted onto the central black hole. We estimated the average energy of escaping protons to be about 100 MeV in order to produce a flux of hard X-ray emission in the energy range 14 – 40 keV as observed by Suzaku/HXD (Yuasa et al. 2008).

The quasi-stationary production rate of subrelativistic protons hardly exceeds $Q \sim 2 \times 10^{45}$ protons s^{-1} for the frequency of star capture $\sim 10^{-5} - 10^{-4}$ years $^{-1}$ (Syer & Ulmer 1999; Donley et al. 2002) and a fraction of escaped matter equaled $\sim 50\%$ of star masses (Ayal et al. 2000).

The unbounded fraction of stars escapes with subrelativistic velocities which correspond energies about 100 MeV for protons and 50 keV for electrons (see Dogiel et al. 2009a). The numbers of protons and electrons equal to each other. Therefore, fluxes of bremsstrahlung hard X-ray emission produced by protons and by electrons equal to each other too. But the lifetime of electrons with energies 50 keV is in about five orders of magnitude smaller than that of 100 MeV protons and the electron bremsstrahlung flux is significant for a short time just after a capture event. Since it is supposed that relatively long time has passed after the last star capture, electron bremsstrahlung radiation is negligible.

Our goal is to estimate the spatial diffusion coefficient, D , of subrelativistic particles near the GC, whose value is unknown. Below we derive its value from the spatial distribution of hard X-ray emission near the GC as observed by Suzaku.

In section 2, we summarize an energetics of the Galactic Center diffuse emission. In section 3, we carry forward our model using non-uniform target gas distribution. Section 4 is devoted to explain how the model and the HXD data can be compared. In section 5 and 6, spatial distribution of 6.7 keV Fe line emission and hard X-ray continuum are compared with ones expected from the present model, deriving a confinement on a diffusion coefficient for the sub-relativistic protons.

2. Components of Hard X-Ray Emission from the GC in the range 14 – 40 keV

Koyama et al. (2007b) reported that the hard X-ray spectrum in the range 2 – 10 keV from the GC is naturally explained by a 6.5 keV-temperature plasma plus a power-law component with the photon index of $\Gamma = 1.4$. Latter on, Yuasa et al. (2008) found a prominent hard X-ray emission in the range from 14 to 40 keV whose spectrum is a power law with the spectral index ranging from 1.8 to 2.5.

Different processes may contribute to the total emission from the GC.

Thermal emission. The emissivity of thermal bremsstrahlung of a hot plasma ε can be estimated from the equation (see e.g. Ginzburg 1989)

$$4\pi\varepsilon = 1.57 \times 10^{-27} n^2(r) \sqrt{T(r)} \text{ erg cm}^{-3} \text{ s}^{-1} \quad (1)$$

where the temperature is in Kelvin degrees.

As follows from the analysis of Suzaku data the plasma temperature in the GC is constant and equals 6.5 keV (Koyama et al. 2007b). Then the thermal emissivity in the GC is

$$4\pi\varepsilon \simeq 1.27 \times 10^{-23} n^2(r) \text{ erg cm}^{-3} \text{ s}^{-1} \quad (2)$$

Dogiel et al. (2009b) presented results of calculation for the $0.55^\circ \times 0.55^\circ$ central region and showed that for the plasma density $n = 0.2 \text{ cm}^{-3}$ and the temperature 6.5 keV the total thermal flux from this region in the energy range 14 – 40 keV was about $F_{\text{th}} \simeq 2 \times 10^{36} \text{ erg s}^{-1}$. The total non-thermal flux was estimated by the value $F_{\text{nth}} \simeq 3 \times 10^{36} \text{ erg s}^{-1}$.

Non-thermal component. Koyama et al. (2009) found that a combination of the Fe XXV- $K\alpha$ and Fe I- $K\alpha$ fluxes was proportional to the non-thermal continuum flux in the 5 - 10 keV energy band. They concluded that the total non-thermal flux consists of the two components, one of which is proportional to the intensity of 6.7 keV line, and, therefore, is produced in regions of hot plasma, while the intensity of the second component is proportional to that of the 6.4 keV line and is generated in regions of molecular gas. Warwick et al. (2006) reported a similar conclusion obtained from the XMM-Newton observations.

In the model of X-ray production by subrelativistic protons this relation is naturally explained (see Dogiel et al. 2009bc). Continuum and line emission is produced in this case by interactions of subrelativistic protons with the background plasma and the molecular hydrogen in the GC.

In spite of relatively small radius ($r \sim 200 \text{ pc}$) the inner Galactic region contains about 10% of the Galaxy's molecular mass, $\sim M_{\text{H}_2} \simeq (7 - 9) \times 10^7 M_\odot$. Most of the molecular gas is contained in very compact clouds (see the review of Mezger et al. 1996). Since the total mass of the molecular gas is much larger than that of the hot plasma, $M_{\text{pl}} \sim 4 \times 10^5 M_\odot$, one may assume that most of inverse bremsstrahlung flux produced by protons would come from regions filled by the molecular gas. However, as Dogiel et al. (2009c) showed, the mean free path of protons in dense molecular clouds is very short since the diffusion coefficient inside molecular clouds is quite small. Therefore, only a small fraction of the molecular hydrogen is involved into processes of inverse bremsstrahlung radiation. Thus, for the molecular cloud Sgr B2 with the mass about $10^6 M_\odot$ it follows from calculations of Dogiel et al. (2009c) and the Suzaku data (see Koyama et al. 2007a) that the total bremsstrahlung flux in the range 2 – 10 keV is about $F_{2-10} \simeq 10^{35} \text{ erg s}^{-1}$. The total flux of the 6.4 keV line emission from Sgr B2 is about $F_{6.4} \sim 1.2 \times 10^{34} \text{ erg s}^{-1}$ that gives the ratio $F_{2-10}/F_{6.4} \sim 8$. For higher energies of X-ray photons our calculations show that the ratio of $F_{14-40}/F_{6.4} \sim 6.4$.

The total flux of the 6.4 keV line from the GC can be estimated from the ASCA data (Maeda 1998) and for the region $0.55^\circ \times 0.55^\circ$ it is about $\sim 1.3 \times 10^{35} \text{ erg s}^{-1}$, then we expect that the total non-thermal bremsstrahlung flux from proton interaction with the molecular gas

is about 10^{36} erg s⁻¹, and 70% of the total non-thermal bremsstrahlung emission in the range 14 – 40 keV, $\sim 2 \times 10^{36}$ erg s⁻¹, is generated in regions filled with the hot plasma.

3. Qualitative effect of the plasma density variations

In this section we present a qualitative effect of plasma density variations on the proton distribution in the GC. We remind that the spatial distribution of subrelativistic protons is described by the quasi-stationary diffusion equation

$$\frac{\partial}{\partial E} (b(E)N) - \nabla D \nabla N = Q(E, \mathbf{r}), \quad (3)$$

where N is the density of cosmic rays, D is the spatial diffusion coefficient, $dE/dt \equiv b(E)$ is the rate of energy losses which for subrelativistic protons is determined by the Coulomb collisions and has the form

$$\left(\frac{dE}{dt} \right)_i = - \frac{4\pi n e^4 \ln \Lambda_1}{m v_p} \simeq \frac{k}{\sqrt{E}}, \quad (4)$$

where v_p is the proton velocity, $\ln \Lambda_1$ is the Coulomb logarithm, and n is the plasma density, which is a function of the radius r in general case. The source function is taken in the form

$$Q(E) = Q \delta(E - E_{\text{esc}}) \delta(\mathbf{r}). \quad (5)$$

where $Q \simeq 3 \times 10^{45}$ protons s⁻¹ and $E_{\text{esc}} \simeq 100$ MeV is the injection energy of protons.

For $n = n_0 = \text{const}$, the spherically symmetric solution is

$$N(r, E) = \frac{Q}{|b(E)| (4\pi\lambda)^{3/2}} \exp \left[-\frac{\mathbf{r}^2}{4\lambda} \right] \quad (6)$$

where

$$\lambda(E) = \int_{E_0}^E \frac{D(E)}{b(E)} dE = \frac{2D}{3k} (E_{\text{esc}}^{3/2} - E^{3/2}) \quad (7)$$

In the case when the plasma density is spatially variable as

$$n(r) = n_0 \left(\frac{r_0}{r} \right)^2, \quad (8)$$

where r_0 is a scale parameter, the analytical solution for $N(r, E)$ is

$$N(r, E) = \frac{Q}{|b(E)| r_0^2 (4\pi\lambda)^{1/2}} \sqrt{\frac{r_0}{r}} \exp \left[-\frac{\lambda(E)}{r_0^2} \right] \exp \left[-\frac{\ln^2(r/r_0) r_0^2}{4\lambda(E)} \right] \quad (9)$$

Here

$$\lambda = \frac{1}{4} \int_{E_0}^E \frac{D(E)}{b(E)} dE \quad (10)$$

In figure 1 we show the difference between uniform for $n_0 = 0.2$ cm⁻³ (solid line) and non-uniform cases for the parameters $n_0 = 10$ cm⁻³ (dashed-dotted line) and $n_0 = 3$ cm⁻³ (dashed line). The scale parameter is taken to be $r_0 = 25$ pc. One can see that variations of the gas density change significantly the proton distribution.

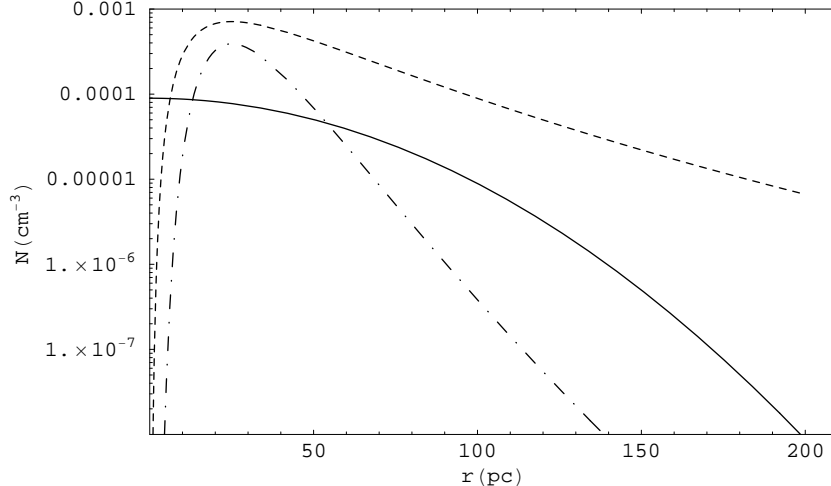


Fig. 1. The spatial distribution of 70 MeV protons in the GC for the case of uniform distribution (solid line) and that of non-uniform distribution equation (9) for $n_0 = 10 \text{ cm}^{-3}$ (dashed-dotted line) and $n_0 = 3 \text{ cm}^{-3}$ (dashed line).

4. How to compare the model calculation and the observed HXD data?

In section 5 and 6, we will compare spectra expected from the present model with the HXD spectrum observed around the GC (Yuasa et al. 2008). Before describing the comparison result, we present methods and assumptions which were used in the calculation.

The intensity I of inverse bremsstrahlung emission of protons in any direction \mathbf{s} is calculated from

$$I(E_x, \mathbf{s}) = \frac{1}{4\pi} \int_{\mathbf{s}} n(r) ds \int_E N(E, r) v \frac{d\sigma_{\text{ib}}}{dE_x} dE \quad (11)$$

where the integration is along the line of sight \mathbf{s} and E_x is the energy of photons. Here $N(E, r)$ is the density of subrelativistic protons with the energy E at the radial distance r from the GC, v is the velocity of protons with the energy E , $d\sigma_{\text{ib}}/dE_x$ is the cross-section of inverse bremsstrahlung radiation, and $n(r)$ is the plasma density distribution in the GC.

To compare such results of our model calculations, which are given in *photons* $\text{cm}^{-2} \text{keV}^{-1} \text{s}^{-1} \text{sr}^{-1}$ with the Suzaku data of Yuasa et al. (2008) given in *counts* s^{-1} , we should convolve the HXD energy and angular responses (see Mitsuda et al. 2007; Takahashi et al. 2007; Kokubun et al. 2007) to the model intensity. The procedure is as follows:

$$f_{14-40} = \int_{\ell, b} d\Omega \int_{14\text{keV}}^{40\text{keV}} dEA(\ell, b) S(E) I(E, \ell, b), \quad (12)$$

where f is in (*counts* s^{-1}) denotes the expected count rate in the direction determined by the galactic coordinates (ℓ, b) , Ω is in (*sr*), $I(E, \ell, b)$ in (*ph* $\text{cm}^{-2} \text{keV}^{-1} \text{s}^{-1} \text{sr}^{-1}$) is the continuum intensity in the direction (ℓ, b) , $S(E)$ and $A(\ell, b)$ represent the effective area and angular transmission of the HXD, respectively.

The HXD data can still include a contaminating flux from a number of X-ray point sources besides the diffuse emission as noted in Dogiel et al. (2009b). The flux level of the contamination is calculated to be on the order of 10% by integrating the known LogN – LogS curve for X-ray point sources around the GC obtained with Chandra (Muno et al. 2009) over the luminosity of $2 \times 10^{32} - 1 \times 10^{34}$ erg s⁻¹ in which range has been actually measured so far (in the "field" region of Muno et al. 2009). Although the contribution can be larger if the LogN – LogS curve is measured further smaller luminosities, in the present comparison with the model calculation, we simply ignore their contribution. The effect of this neglect is discussed later in section 6.

5. Spatial Variations of the Gas Density in the GC

The spatial distribution of the hot plasma in the GC can be derived from the distribution of the 6.7 keV iron line which traces the hot plasma.

The origin of the K- α iron line from the hot plasma of the GC is pure thermal (see Dogiel et al. 2009b). Then for the surface brightness distribution of the 6.7 keV emission line in any direction \mathbf{s} to the GC we have

$$I_{6.7}(\mathbf{s}) \propto \int_{\mathbf{s}} n^2(r) ds \quad (13)$$

Maeda (1998) obtained a surface brightness distribution of the 6.7 keV emission line, $I_{6.7}$, from the ASCA data as a function of the angle from the Galactic center, θ ,

$$I_{6.7}(\ell, b) = I_1 \exp\left(-\frac{|\theta|}{\omega_1}\right) + I_2 \exp\left(-\frac{|\theta|}{\omega_2}\right) \quad (14)$$

$$\cos \theta = \cos \ell \cos b$$

where θ is the angle from $(\ell, b) = (0, 0)$, $I_1=19.7$ and $I_2=1.6$ in *photons cm⁻²s⁻¹sr⁻¹* units, and $\omega_1 = 0.42$ and $\omega_2 = 15$ in degrees.

This distribution is shown in figure 2 by the thick solid line.

From the 6.7 line distribution of Maeda (1998) we try to derive the plasma density distribution in the GC. Then we will use this density distribution for calculations of hard X-ray emission from the GC. We represent the hot plasma distribution by analytical functions as

$$n(r) = n_0 \exp\left[-\frac{1}{2}\left(\frac{r}{r_0}\right)^\alpha\right], \quad (15)$$

and our goal is to find suitable parameters r_0 and α which give good correspondence of the observed ASCA data and that obtained with the density distribution (15).

In order to derive the model spatial variations of the 6.7 keV line emission along the Galactic plane we should integrate along the direction \mathbf{s} shown in figure 3. The angle between the direction to the GC and the line of view is the Galactic longitude ℓ . The circle line around the Galactic center defines a sphere filled with a hot plasma whose radius is supposed to be about $a = 200$ pc in accordance with the X-ray observations (see, e.g. Koyama et al. 1996).

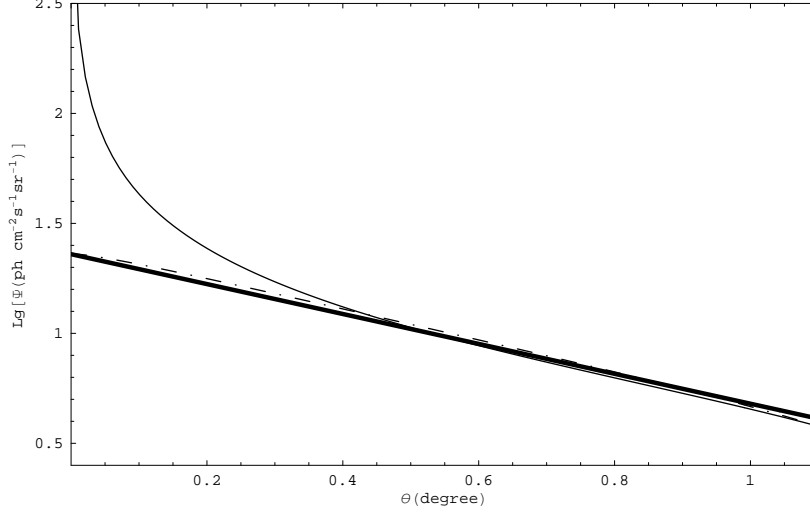


Fig. 2. The latitude distribution of 6.7 keV line as from the ASCA data by Maeda (1998) is shown by the solid line. Model spatial distribution of the surface brightness profile of the 6.7 keV emission line expected from equation (17) for plasma distributions: $r_0 = 25$ pc and $\alpha = 0.7$ (dashed-dotted line), and uniform plasma distribution (thin solid line).

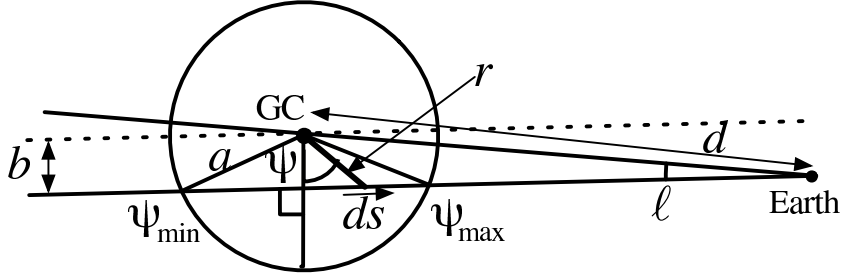


Fig. 3. The schematic view of the GC from Earth. The arrow line shows the distance between Earth and the GC, the solid line is the line of view, the solid circle shows the region of hot plasma around the GC; the two radius-vectors mark positions of ψ_{\max} and $\psi_{\min} = \pi - \psi_{\max}$.

The radius-vector r from the GC along the line of sight as a function of the Galactic longitude ℓ and the angle ψ between the line coinciding Earth and the GC (arrow line) is described as

$$r(\ell, \psi) = d \cdot \frac{\sin \ell}{\cos \psi} \quad (16)$$

Then with the density distribution (15) the integration along the line of sight in the direction s is

$$I_{6.7} \propto \int_{\pi - \psi_{\max}}^{\psi_{\max}} n^2(r(\ell, \psi)) \frac{ds}{d\psi} d\psi \quad (17)$$

where

$$\frac{ds}{d\psi} = -a \cdot \frac{\cos \psi_{\max}}{\cos^2 \psi} \quad (18)$$

and the angles $\pm\psi_{\max}$ shown by the two radius-vectors in figure 3 is

$$\psi_{\max} = \arccos \left[\frac{d}{a} \sin \ell \right] \quad (19)$$

Here $d = 8$ kpc is the distance between Earth and the GC which equals 8 kpc (Reid 1993). From equation (17) and the ASCA 6.7 keV spatial variations obtained by Maeda (1998) we derived parameters r_0 and α , that gives $r_0 = 25 - 75$ pc and $\alpha = 0.7 - 1.7$. The ASCA spatial variations of 6.7 keV line are shown in figure 2 by the thick solid line. As an example we show also in this figure the model spatial variations of the 6.7 keV line intensity derived for $r_0 = 25$ pc and $\alpha = 0.7$ (dashed-dotted line). The coincidence between calculations and data are reasonably good. For comparison we showed also in this figure the expected 6.7 keV line spatial variation for the case of uniform plasma distribution (thin solid line). One can see that the ASCA data can hardly be described by a model with the uniform plasma distribution.

The parameter n_0 of equation (15) can be roughly estimated by comparing the model emission (6.5 keV thermal + non-thermal) with the observed spectrum of the hard X-ray emission around the GC (Yuasa et al. 2008). To perform such a comparison, we convolved the model spectrum with the HXD response as described in section 4, and then, overlaid it over the HXD spectrum by adjusting the model normalization factor, n_0 in equation (15), so that the model reproduces the HXD fluxes. Figure 4(a) shows a result of the convolution, and the model well reproduce the observed spectrum in the 14 – 40 keV band. Although we only present the result for one parameter set explained in the caption of figure 4, the model spectral shape does not strongly depend on the parameters, and within possible parameter ranges, n_0 was calculated to be $\sim 0.1 - 0.3 \text{ cm}^{-3}$.

As one can see from these figures the contributions of thermal and non-thermal emission into the total flux from the GC are almost equal to each other in this energy range (their ratio is 2:3).

6. Diffusion Coefficient of Cosmic Rays in the Galactic Center

In order to calculate the spatial distribution of subrelativistic protons in the GC we should take into account energy losses in regions of hot plasma and in the regions of neutral gas surrounding the GC whose average density was taken to be $n_H = 1 \text{ cm}^{-3}$.

As follows from the analysis of Yuasa et al. (2008) the spatial distribution of the intensities of thermal and non-thermal emission in the GC are similar to each other. Since the first one is proportional $I_{\text{th}} \propto \int_r n^2(r) ds$ and the second one is proportional to $I_{\text{nth}} \propto \int_r n(r) N_p(r) ds$, where $N_p(r)$ is the spatial distribution of subrelativistic protons, it means that the spatial distribution of subrelativistic protons does not differ strongly from that of plasma.

The expected spatial distributions of the 14 – 40 keV X-ray emission in the GC derived from equation (11) for $D = 3 \times 10^{25} \text{ cm}^2 \text{ s}^{-1}$ (solid line) and for $D = 3 \times 10^{26} \text{ cm}^2 \text{ s}^{-1}$ (dashed line)

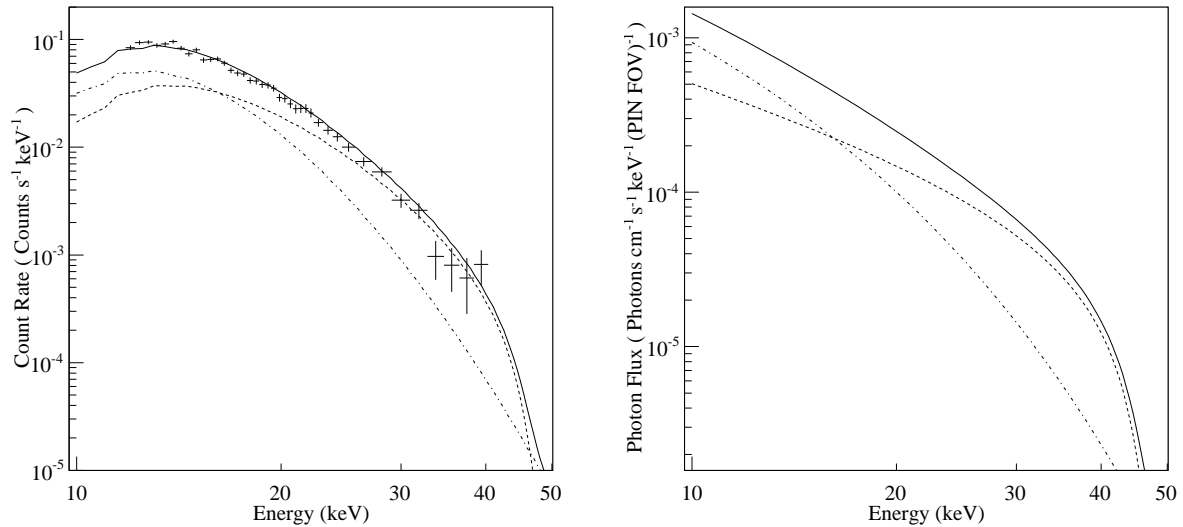


Fig. 4. (a) The 14 – 40 keV X-ray spectrum observed by HXD/PIN around the GC (taken from Yuasa et al. 2008). The model spectra for 6.5 keV thermal emission, inverse bremsstrahlung, and sum of them are also shown in dashed, dashed-dotted, and solid line. The model spectra were calculated using such parameters as $r_0 = 50$ pc, $\alpha = 1.1$, $D = 1 \times 10^{26}$ cm²/s, and $n_0 = 0.13$ cm⁻³. (b) The same model spectra as (a) are shown without convolving the HXD/PIN energy response but with integration over the PIN FOV (0.55×0.55 , effectively).

and the Suzaku data obtained by Yuasa et al. (2008) are shown in figure 5¹. Our calculations show that spatial distribution of the non-thermal 14 – 40 keV X-ray emission does not differ significantly from each other. However, the necessary proton production rate Q is an essential function of the diffusion coefficient. Thus, for $D = 3 \times 10^{25}$ cm²s⁻¹ the value of Q needed to reproduce the Suzaku data equals 10^{45} protons s⁻¹ while for $D = 3 \times 10^{26}$ cm²s⁻¹ the production rate is necessary to be $Q = 2.3 \times 10^{45}$ protons s⁻¹. We remind that the average rate of proton production by accretion on the black hole is no more than $Q = 3 \times 10^{45}$ protons s⁻¹. Since the value of Q is restricted, then permitted values of D are confined within a relatively narrow range around $D \simeq 10^{26}$ cm² s⁻¹.

However, these estimates were obtained in assumption that almost 100% of the 14 – 40 keV X-ray flux from the GC is generated by subrelativistic protons. As follows from, e.g., Warwick et al. (2006); Revnivtsev et al. (2009) a significant part of the GC hard X-ray flux may be due to faint point sources. Then a smaller production rate of protons in the GC is required, and, hence, higher values of the diffusion coefficient cannot be excluded.

¹ In figure 5, the data point at $l = 0.55$ is largely discrepant from the model, and even from the other data points. As noted in Yuasa et al. (2008), this deviation could be due to underestimation of contaminating signals from known bright point source inside the HXD/PIN FOV. Therefore, this point should be ignored in the present comparison between observed data and the model calculation.

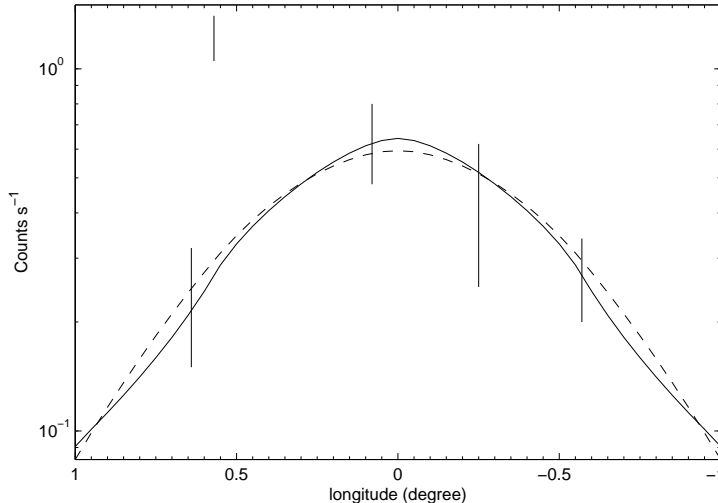


Fig. 5. The spatial distribution of inverse bremsstrahlung flux in the energy range 12 – 40 keV averaged over the HXD field of view with the Suzaku data. Solid line: $D = 3 \times 10^{25} \text{cm}^2 \text{s}^{-1}$, $Q = 10^{45} \text{protons s}^{-1}$. Dashed line: $D = 3 \times 10^{26} \text{cm}^2 \text{s}^{-1}$, $Q = 2.3 \times 10^{45} \text{protons s}^{-1}$. The Suzaku data were taken from Yuasa et al. (2008)

7. Discussion and Conclusion

Analysis of X-ray data (Koyama et al. 2009) demonstrated that continuum non-thermal emission in the GC consisted of two components one of which was proportional to the intensity of 6.7 keV iron line which traced distribution of hot 6.5 keV plasma, and the other one was proportional to the intensity of 6.4 keV plasma which traced distribution of cold molecular hydrogen. If this non-thermal emission is due to inverse bremsstrahlung emission of subrelativistic protons, then their interactions with hot and cold fractions of the interstellar medium are equally important. Our estimation show that about 30% of the total non-thermal flux from the GC in the range 14 – 40 keV is generated in regions of cold gas while the rest is produced by proton interaction with hot plasma. The reason is that only a small fraction of molecular gas is involved into processes of bremsstrahlung emission because of short mean free path of protons in molecular clouds.

From the X-ray data obtained with ASCA (Maeda 1998) it was concluded that the plasma density distribution in the GC is strongly non-uniform, e.g. the model distribution of 6.7 keV line in the GC obtained with the plasma profile

$$n(r) = 0.2 \times \exp \left[- \left(\frac{r}{50(\text{pc})} \right)^{1.1} \right] (\text{cm}^{-3}) \quad (20)$$

is very close to that from ASCA observation. This effect of density variations should be included into analysis of protons propagation in the GC.

From the total spectrum of X-ray emission in the range 14 – 40 keV from the 0.55°-

diameter central region and the spatial variation of this emission within 1.5° -diameter central region as observed by Suzaku and ASCA we derived the characteristic diffusion coefficient of subrelativistic protons. It was shown that the diffusion coefficient of subrelativistic particles is about the value of $3 \cdot 10^{26} \text{ cm}^2 \text{ s}^{-1}$. For higher values of the diffusion coefficient a higher production rate of subrelativistic protons is necessary which cannot be provided by accretion. However, this estimation of D one should consider as a lower limit. The point is that we assumed here that all hard X-ray emission in the 14–40 keV band is produced by subrelativistic protons in the hot fraction of the interstellar gas. However as stated above a part of this emission may be produced in molecular clouds. Besides, we do not know exactly which part of this emission is due to unresolved point sources (see discussion in Dogiel et al. 2009b). Therefore, we cannot exclude that the diffusion coefficient in the GC is close to its average value in the Galaxy, i.e. $D \sim 10^{27} \text{ cm}^2 \text{ s}^{-1}$. Thus, we determine the range of values of the diffusion coefficient in the GC as $10^{26} - 10^{27} \text{ cm}^2 \text{ s}^{-1}$.

The authors are grateful to the referee, Prof. Fumiaki Nagase, for his comments and corrections.

VAD and DOC were partly supported by the RFBR grant 08-02-00170-a, the NSC-RFBR Joint Research Project No 95WFA0700088 and by the grant of a President of the Russian Federation "Scientific School of Academician V.L.Ginzburg". KSC is supported by a RGC grant of Hong Kong Government under HKU 7014/07P. A. Bamba is supported by JSPS Research Fellowship for Young Scientists (19-1804). CMK is supported in part by National Science Council, Taiwan under the grant NSC-96-2112-M-008-014-MY3.

References

- Ayal, S., Livio, M., & Piran, T. 2000, ApJ, 545, 772
 Cheng, K. S., Chernyshov, D. O., & Dogiel, V. A. 2006, ApJ, 645, 1138.
 Cheng, K. S., Chernyshov, D. O., & Dogiel, V. A. 2007, A&A, 473, 351.
 Dogiel, V.A., Cheng, K.-S., Chernyshov, D.O. et al. 2008, New Astronomy Reviews, 52, 460
 Dogiel, V. A., Tatischeff, V., Cheng, K.-S., et al. 2009a, A&A, submitted
 Dogiel, V., Chernyshov D., Yuasa, T. et al. 2009b, PASJ, submitted
 Dogiel, V. A., Cheng, K-S., Chernyshov, D.O. et al. 2009c, PASJ, to be published in PASJ, 61, No.5
 Donley, J. L., Brandt, W. N., Eracleous, M., & Boller, Th. 2002, ApJ, 124, 1308.
 Ginzburg, V.L. 1989, *Applications of Electrodynamics in Theoretical Physics and Astrophysics*, Gordon and Brech Science Publication.
 Kokubun, M., Makishima, K., Takahashi, T. et al. 2007, PASJ, 59, 53
 Koyama, K., Maeda, Y., Sonobe, T. et al. 1996, PASJ, 48, 249
 Koyama, K., Inui, T., Hyodo, Y. et al. 2007a, PASJ, 59, 221
 Koyama, K., Hyodo, Y., Inui, T. et al. 2007b, PASJ, 59, S245

Koyama, K., Takikawa, Y., Hyodo, Y. et al. 2009, PASJ, 61, S255
Maeda, Y. 1998, Ph.D. Thesis
Mezger, P. G., Duschl, W. J., & Zylka, R. 1996, Astro.Astrophys.Rev., 7, 289
Mitsuda, K., Bautz, M., Inoue, H. et al. 2007, PASJ, 59, S1
Muno, M.P., Bauer, F.E., Baganoff, F.K. et al. 2009, ApJS, 181, 110
Reid, M. J. 1993, ARA&A, 31, 345
Revnivtsev, M., Sazonov, S., Churazov, E. et al. 2009 Nature, 458, 1142
Syer, D., & Ulmer, A. 1999 MNRAS, 306, 35
Takahashi, T., Abe, K., Endo, M. et al. 2007, PASJ, 59, 35
Warwick, R., Sakano, M., & Decourchelle, A. 2006, Journal of Physics Conference Series, 54, 103
Yuasa, T., Tamura, K., Nakazawa, K. et al. 2008, PASJ, 60, S207